Kobe University Repository : Kernel

PDF issue: 2025-12-05

Structural Modification along Heavy Ion Tracks in Poly(allyl diglycol carbonate) Films

Yamauchi, Tomoya ; Mori, Yutaka ; Oda, Keiji ; Yasuda, Nakahiro ; Kitamura, Hisashi ; Remi, Barillon

(Citation)
Japanese Journal of Applied Physics,47(5):3606-3609

(Issue Date)
2008

(Resource Type)
journal article

(Version)
Accepted Manuscript

(Rights)
© (公社)応用物理学会 2008

(URL)
https://hdl.handle.net/20.500.14094/90001393

Structural Modification along Heavy Ion Tracks in Poly(allyl Diglycol Carbonate) Films

Tomoya Yamauchi, Yutaka Mori, Keiji Oda, Nakahiro Yasuda [1],
Hisashi Kitamura [1], Rémi Barillon [2]

Graduated School of Maritime Sciences, Kobe University, Kobe 658-0022, Japan
[1] National Institute of Radiological Science, Chiba 263-8555, Japan
[2] Institut Plurisdisciplinaire Hubert Curien (UMR 7178), 67037 Strasbourg Cedex 2, France

To identify the chemical modifications along nuclear tracks in poly(allyl diglycol carbonate) (PADC), we have made a series of Fourier transform infrared (FT-IR) measurements for films with a thickness of about 3 μm that have been exposed to C, Ne, Ar, and Fe ions in air. The amount of carbonated ester bonds lost due to the exposure was estimated from the changes in the absorbance of C=O and C-O-C bonds with the heavy ion fluence. The G-value for the breaking of carbonate ester bonds and the corresponding track core radii were obtained as a function of stopping power. The calculated radial dose distribution indicated that the core was formed at regions where the local dose was higher than 10^6 Gy.

Keywords: SSNTD, latent track, track core, PADC, CR-39, FT-IR, G-value

1. Introduction

Poly(allyl diglycol carbonate)(PADC), which is known under the trade name CR-39, is a commonly used solid state nuclear track detector (SSNTD) in different branches of science and technology such as nuclear physics, cosmic rays, dosimetry in space, neutron dosimetry, radiation biology, and the strengthened safeguard system [1)]. About three decades have passed since the discovery of CR-39 plastic as a SSNTD material [2)]. There remain some unresolved aspects, however, of the latent track formation process in this material [3)]. Only a few studies have been carried out on the radial size and modified chemical structure of the latent tracks. The effect of dissolved oxygen on the sensitivity has been noted, but the corresponding chemical process in the tracks has not beenyet resolved. In addition to the fundamental interest, much more sensitive SSNTDs which can record protons recoiled by neutrons up to 100 MeV are needed in the filed of neutron dosimetry, similar to the recently developed fluorescent nuclear track detector using aluminum oxide [4)]. On the other hand, an SSNTD material with a sufficient threshold and high charge resolution for heavy ions has been also sought to measure the composition of the heaviest elements in galactic cosmic rays [5)]. Generally speaking, polymers have an advantage in producing detectors with wide areas of uniform quality. Because PADC is one of the most sensitive polymeric track detectors, information on the track structure and the track formation process in it will be helpful for the development of a novel SSNTD with a controllable sensitivity and detection threshold level.

In the case of an etched track detector, the tracks are characterized by the track etching rate, which is the penetrating speed of an etching solution along a latent track. Etch pits, which can be observed under an optical microscope, are formed when the track etching rate is greater than the bulk etching rate. The latent tracks are expected to have a certain nano-scale structure in the radial direction [6)]. The heavily damaged center region, i.e. track core, should be surrounded by a slightly modified circular transition area, i.e. track halo or penumbra, which is connected to the original unaffected region. Several kinds of experimental methods have been briefly summarized in the literature for latent tracks in polymer materials [6)]. Among them conductometry has been an effective and widely applied method to study the nuclear tracks in various kinds of polymers [7-9)]. According to this method, one can determine the radial-track-etch-rate, which is the penetrating speed of an etching solution in the radial direction around the track core and halo even for a single track. Since the radial-track-etch-rate can be expected to reflect the local energy density deposited by a heavy ion, it should be useful not only to evaluate the track core size but also to examine the damage distribution

around the ion path. The track core may be treated as a central region where the etch rate is significantly enhanced. In some types of polymer, a reduction in the etch rate was observed in the halo [9, 10]. The role of segmented and diffused small molecules which were produced in the track core in forming the halo was discussed [10]. Recently, a conductmetric study was reported for PADC films [11]. Transmission electron microscope (TEM) observations on a replica of slightly etched tracks also gave information on the structure of submicron damage in nuclear tracks [12, 13]. These methods gave us some important knowledge about tracks but could not provide any information on chemical modifications caused around the latent tracks. When we consider new SSNTDs, we need to know the chemical structure of the damage around the nuclear tracks.

For the purpose of understanding the modified chemical structure along heavy ion tracks in polymer films, Fourier transform infrared (FT-IR) spectrometry is an available method for both qualitative and quantitative analyses, and many studies have been performed on various kinds of polymers [14-18]. Several FT-IR studies have also been carried out on PADC; however, quantitative analyses have been insufficient [19-22]. The authors have studied the loss of ether bonds along carbon ion tracks in 15-μm-thick PADC films [23]. Recently, we succeeded in preparing thinner PADC films with thicknesses ranging from 1.7 to 5 μm, which enabled us to obtain unsaturated infrared absorption spectra (IR spectra), including carbonate ester bonds [24].

In this study, the prepared PADC films were exposed to accelerated C, Ne, Ar, and Fe ions, at incident energies around the Bragg peaks in air. The damage density, qualified by the loss of carbonate ester bonds per unit length of the ion tracks, was evaluated based on the changes in the relative absorbance of the peaks in FT-IR spectra with ion fluence. The G-value for the loss of carbonate ester bonds and the corresponding track core radius were also determined. The radial dose distributions were calculated to evaluate the locally deposited energy where track cores were formed.

2. Experiments

Figure 1 shows the repeat unit of PADC. It has an ether bond in the center and two carbonate ester bonds in symmetrical positions. Thin PADC films with a thickness of about 3 μm were prepared by chemical etching from commercially obtained pure sheets with a nominal thickness of 100 μm (BARYOTRAK, Fukuvi Chemical Industry). After etching in 6 M KOH solution kept at 70 ˚C, the films were carefully rinsed in distilled water and then dried in a clean and dark place after the excess water was removed [24]. Heavy ion exposure was carried out in the air utilizing the medium energy irradiation system of heavy ion medical accelerator in Chiba (HIMAC), NIRS, Japan [25].

The irradiation conditions are shown in Table 1. The electronic stopping power, that is also called the unrestricted linear energy transfer, is presented as the average value inside the films as calculated by SRIM code [26]. Overlapping of ion tracks can be ignored under these fluences. FT-IR measurements were performed for each film examined both before and after the irradiation using a spectrometer FT/IR-6100S (JASCO), the entire system of which can be evacuated, including the interferometer, photon-detector, and sample room, during the measurements. The thickness of each film was evaluated from the net absorbance of typical bonds based calibration curves [24].

3. Results and Discussion

Figure 2 shows IR spectra of PADC films with a thickness of 3 μm before and after 147 MeV Fe ion irradiation at a fluence of 1.5×10^{11} ions/cm^2. The absorption bands of carbonate ester bonds at 1745 cm^{-1}, C=O, and at 1260 cm^{-1}, C-O-C, apparently decrease in intensity after the exposure. Assignment of absorption bands in the IR region of PADC has been well summarized in the literature [24]. Their values of absorbance are greater than 1.0, but we have previously confirmed that these are fairly proportional to the film between 1.7 and 5.0 μm thick for un-irradiated films [24]. Then we advanced our analysis based on the Lambert-Beer law in this study. The observed reductions of peak height resulted from the formation of latent tracks. The relative absorbance, A/A_0, was obtained at all the fluences examined for each ion, where A is the net absorbance of the considered bands after the irradiation, and A_0 is that before irradiation. In this case, the relative absorbance is equal to the survival fraction, N/N_0, that is the ratio of the number density of the bonds of interest after the irradiation, N, to that of the original ones, N_0;

$$\frac{A}{A_0} = \frac{N}{N_0}. \qquad (1)$$

The results for C=O bonds are shown in Fig. 3, in which A/A_0 is plotted against the fluence, F, for the four ions. From these observations, we were able to derive the following experimental relation for each ion,

$$\frac{N}{N_0} = 1 - \sigma_i \cdot F, \qquad (2)$$

where F is in the unit ions/cm^2 and σ_i is an experimental constant for the i th ion in units of cm^2 [16]. This form of equation was expected at fluences where track overlap is negligible. The constant σ_i is the effective track core area in where C=O were lost. With increasing ion charge, the track core area becomes apparently larger, as shown in Fig. 3. Concordant results were attained from changes in the absorption of the C-O-C

band in the carbonate ester bonds.

The damage density, taken as the loss of carbonate ester bonds per unit length of the heavy ion track, was calculated as the product of the number density of the bonds and the effective track core area [23]. Figure 4 indicates the damage density determined from the scissions of C=O and C-O-C bonds for four ions as a function of the average stopping power in the films. Solids symbols indicate the values evaluated from the C=O band and the open ones from the C-O-C band; both give the equivalent results. As indicated in Fig. 4, the damage density increases sharply with an increase in the stopping power. The G-values for the loss of the carbonate ester bond (loss/100 eV) were calculated by dividing the stopping power into the damage density. In Fig. 5, the G-value is plotted against the average stopping power. It is observed that the G-value is clearly dependent on the stopping power. This is in agreement with a similar trend previously reported for other polycarbonate films [17, 18].

As a first approximation, the geometry of the track core was modeled as a damaged cylinder with cross sectional area σ_i, from which we can evaluate the effective track core radius, r_i. This means that we hypothesized that all carbonate ester bonds inside the cylinder were broken. We then derived the effective track core radius, r_i, using the simple relation

$$r_i = \sqrt{\frac{\sigma_i}{\pi}}. \qquad (3)$$

Figure 6 shows the effective track core radius plotted against the average stopping power. The broken curve indicates the results from the ultraviolet (UV) method, in which the core size was determined from the dependence of UV absorption spectra on the ion fluence based on the track-overlapping model [27]. Our results from FT-IR spectra are concordant with the previous ones shown in this figure. In contrast, the core radius assessed from curves for the evolution of pit-opening during short time etching using an atomic force microscope (AFM) had slightly larger values in comparison to the spectral methods [27]. Conductmetric studies and TEM studies on the replica also showed a relatively large core size compared with those from FT-IR studies in bisphenol A polycarbonate films [10, 12, 13, 17, 18]. This difference may be important to understand the early stages of the chemical etching.

According to the radial-dose-distribution theory for ion tracks [28], the local dose distributions for the four ions were calculated and are presented in Fig. 7. In this calculation, the ionizing potential was assumed to be I = 70.1 eV. Solid symbols on the dose distribution curves are for each track core radius obtained in this FT-IR study. Based on this model, we conclude that the core was formed at regions where the local

dose was higher than approximately 10^6 Gy. Based on the radial-dose-distribution theory according to ref. 28, we can understand the observed dependence of G-values on ion species or stopping power.

4. Closing Remarks

In our previous studies on the tracks of C and Fe ions in PADC, we found the track core radii for loss of carbonate ester bonds and ether bonds were almost equivalent. The results indicated that the parts between two carbonate ester bonds in each repeat unit were segmented into small molecules composed of one or two carbon atoms, including CO_2, formed by breaking the ether bonds and carbonate ester bonds [23, 24]. Such relatively long segmentation indicated that PADC may be an excellent track detector material. Etchants need a certain critical size of track core radius to penetrate along it in track etching. Low-LET radiations and high-energy protons hardly cause such segmentation because of their low ionization densities (see the local dose distribution of 1 MeV proton in Fig. 7). Since the length of the PADC monomer is about 2 nm, segmentation must have occurred in several neighboring repeat units in the radial direction along the heavy ion tracks that were examined in this study.

What is important in forming the etchable tracks in SSNTDs should not be the simple scission of polymeric chains but multi-scissions forming vacant volumes a few nanometers in size. In order to enhance the sensitivity of polymeric SSNTD, the number density of radiosensitive bonds like ether bonds or carbonate ester bonds should be increased. On the other hand, we might be able to determine the detection threshold by changing the distance between neighboring radiosensitive bonds, for example, two carbonate ester bonds connected by a radio-insensitive segment. We are now designing polymeric SSNTDs that may have greater sensitivity than PADC.

Acknowledgements

The authors express our thanks to the staff of NIRS-HIMAC for their support during the experiments (p138). This work was made as a part of the Research Project with Heavy Ions at NIRS-HIMAC.

References

1) D. Nikezic and K. N. Yu: Mater. Sci. Eng. R. **46** (2004) 51.

2) B. G. Cartwright, E. K. Shirk, and P. B. Price: Nucl. Instrum. Methods **153** (1978) 457.

3) T. Yamauchi: Radiat. Meas. **36** (2003) 73.

4) G. M. Akselrod, M. S. Akselrod, E. R. Benton, and N. Yasuda: Nucl. Instrum. Methods Phys. Res., Sect. B **247** (2006) 295.
5) A. J. Westphal, P. B. Price, B. A. Weaver, and V. G. Afanasiev: Nature **396** (1998) 50.
6) W. Enge: Radiat. Meas. **25** (1995) 11.
7) C. P. Bean, M. V. Doyle, and G. Entine: J. Appl. Phys. **41** (1970) 1454.
8) F. Peterson and W. Enge: Radiat. Meas. **25** (1995) 43.
9) P. Apel, A. Schulz, R. Spohr, C. Trautmann, and V. Vustadakis: Nucl. Instrum. Methods Phys. Res., Sect. B **146** (1998) 468.
10) P. Yu. Apel, A. P. Akimenko, I. V. Blonskaya, T. Cornelius, R. Neumann, K. Schwarts, R. Spohr, and C. Trautmann: Nucl. Instrum. Methods Phys. Res., Sect. B **245** (2006) 284.
11) V. R. Oganesyan, V. V. Trofimov, S. Gaillard, M. Fromm, M. Danziger, D. Hermsdorf, and O. L. Orelovitch: Nucl. Instrum. Methods Phys. Res., Sect. B **236** (2005) 289.
12) D. H. Francisco, L. Vanni, O. A. Bernaola, G. Saint Martin, and A. Filevich: Nucl. Instrum. Methods Phys. Res., Sect. B **218** (2004) 461.
13) O. A. Bernaola, G. Saint Martin, and S. M. Azpiazu Garrido: Radiat. Meas. **41** (2006) 247.
14) E. Balanzat, N. Betz, and S. Bouffard: Nucl. Instrum. Methods Phys. Res., Sect. B **105** (1995) 46.
15) Y. Hama, K. Hamanaka, H. Matsumoto, H. Kudoh, T. Sasuga, and T. Seguchi: Radiat. Phys. Chem. **46** (1995) 819.
16) R. Barillon and T. Yamauchi: Nucl. Instrum. Methods Phys. Res., Sect. B **208** (2003) 336.
17) Y. Sun, Z. Zhu, Z. Wang, Y. Jin, J. Liu, M. Hou, and Q. Zhang: Nucl. Instrum. Methods Phys. Res., Sect. B **209** (2003) 188.
18) F. Dehaye, E. Balanzat, E. Ferain, and R. Legras: Nucl. Instrum. Methods Phys. Res., Sect. B **209** (2003) 103.
19) C. Gagnadre, J. L. Decossas, and J. C. Vareille: Nucl. Instrum. Methods Phys. Res., Sect. B **73** (1993) 48.
20) T. Phukan, D. Kanjilal, T. D. Goswami, and H. L. Das: Radiat. Meas. **36** (2003) 611.
21) Z. Lounis-Mokrani, M. Fromm, R. Barillon, A. Chambaudet, and M. Allab: Radiat. Meas. **36** (2003) 615.
22) D. Fink, ed.: Fundamentals of Ion-Irradiated Polymers: Mater. Sci. **vol. no. 63**, (2004) Springer, p. 290.
23) T. Yamauchi, R. Barillon, E. Balanzat, T. Asuka, K. Izumi, T. Masutani, and K. Oda:

Radiat. Meas. **40** (2005) 224.
24) T. Yamauchi, S. Watanabe, A. Seto, K. Oda, N. Yasuda, and R. Barillon: Radiat. Meas. in press.
25) N. Yasuda, T. Konishi, K. Matsumoto, T. Yamauchi, T. Asuka, Y. Furusawa, Y. Sato, K. Oda, H. Tawara, and K. Hieda: Radiat. Meas. **40** (2005) 384.
26) http://www.srim.org/
27) T. Yamauchi, N. Yasuda, T. Asuka, K. Izumi, T. Masutani, K. Oda, R. Barillon: Nucl. Instrum. Methods Phys. Res., Sect. B **236** (2005) 318.
28) M. P. R. Waligórski, R. N. Hamm, and R. Katz: Nucl. Tracks Radiat. Meas. **11** (1986) 309.

Figure captions

Fig. 1 Repeat unit of PADC.

Fig. 2 FT-IR spectra of 3 μm PADC films before and after exposure to Fe ions.

Fig. 3 Decrease of carbonate ester bonds with heavy ion fluence.

Fig. 4 Loss of carbonate ester bonds per unit length of ion tracks, damage density, as a function of the average stopping power of the PADC films. The values of solid symbols were estimated from C=O and the open ones from C-O-C.

Fig. 5 G-values for the loss of carbonate ester bonds with the average stopping power. The values of solid symbols were estimated from C=O and the open ones from C-O-C.

Fig. 6 Effective track core radius for the loss of carbonate ester bonds. The values of solids symbols were estimated from C=O and the open ones from C-O-C.

Fig. 7 Radial dose distribution of energy deposited around the path of heavy ions and protons in PADC. In this calculation the ionizing potential was set at I = 70.1 eV.

Table 1 Conditions of heavy ion irradiation.

Ion	Incident energy (MeV)	Stopping power (keV/μm)	Fluence (ions/cm^2)
C-12	25	653	1.5×10^{12} - 4.0×10^{12}
Ne-20	24	1790	3.5×10^{11} - 6.0×10^{11}
Ar-40	46	3880	1.0×10^{11} - 3.0×10^{11}
Fe-56	147	5151	8.0×10^{10} - 1.5×10^{11}

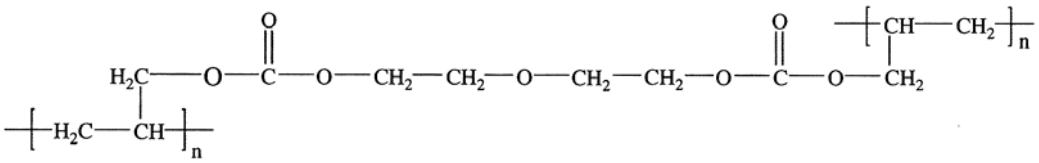

Fig. 1 Repeat unit of PADC.

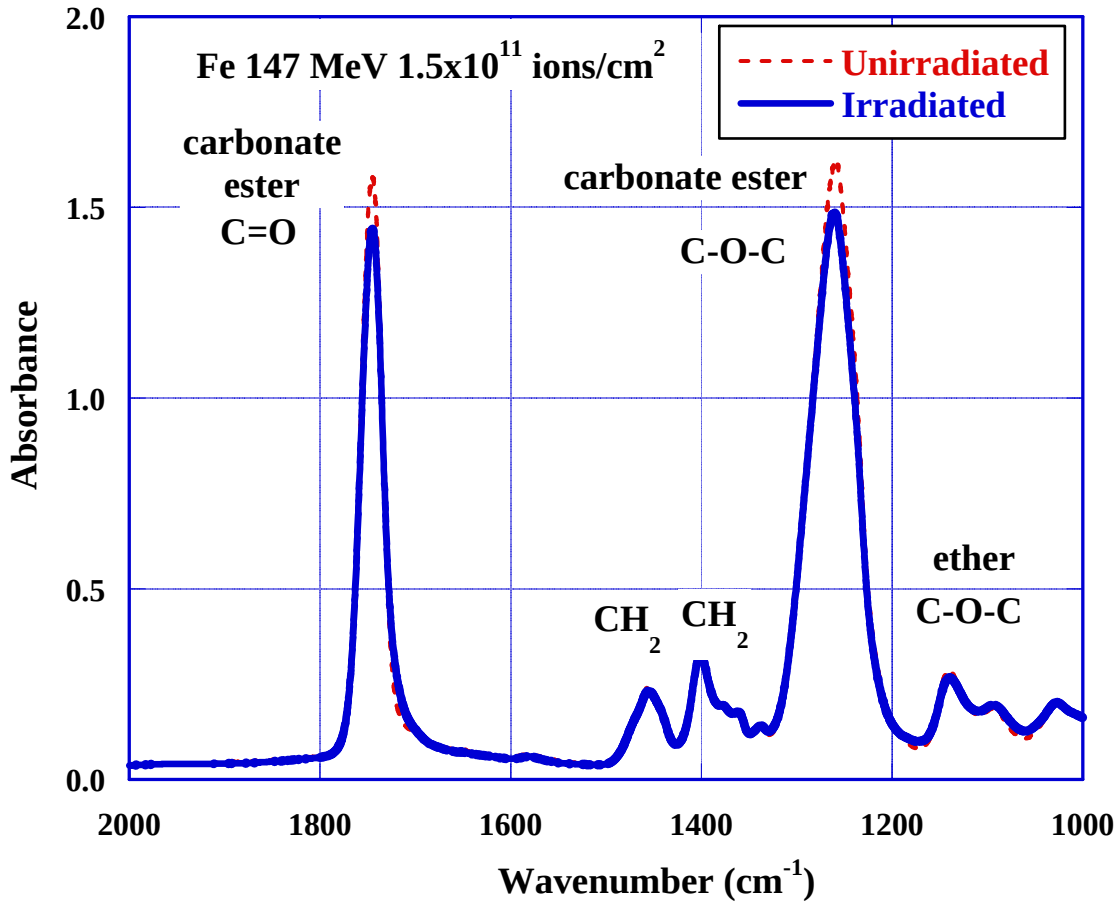

Fig. 2 FT-IR spectra of 3 μm PADC films before and after exposure to Fe ions.

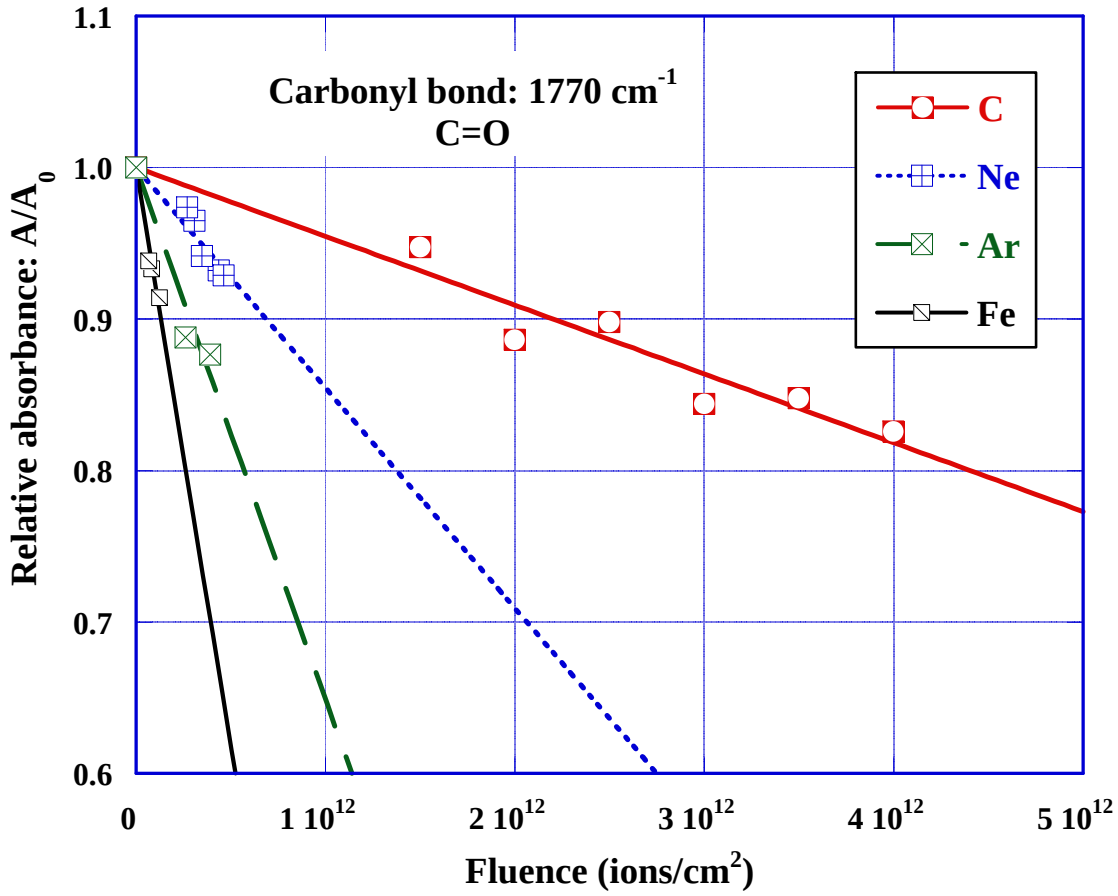

Fig. 3 Decrease of carbonate ester bonds with heavy ion fluence.

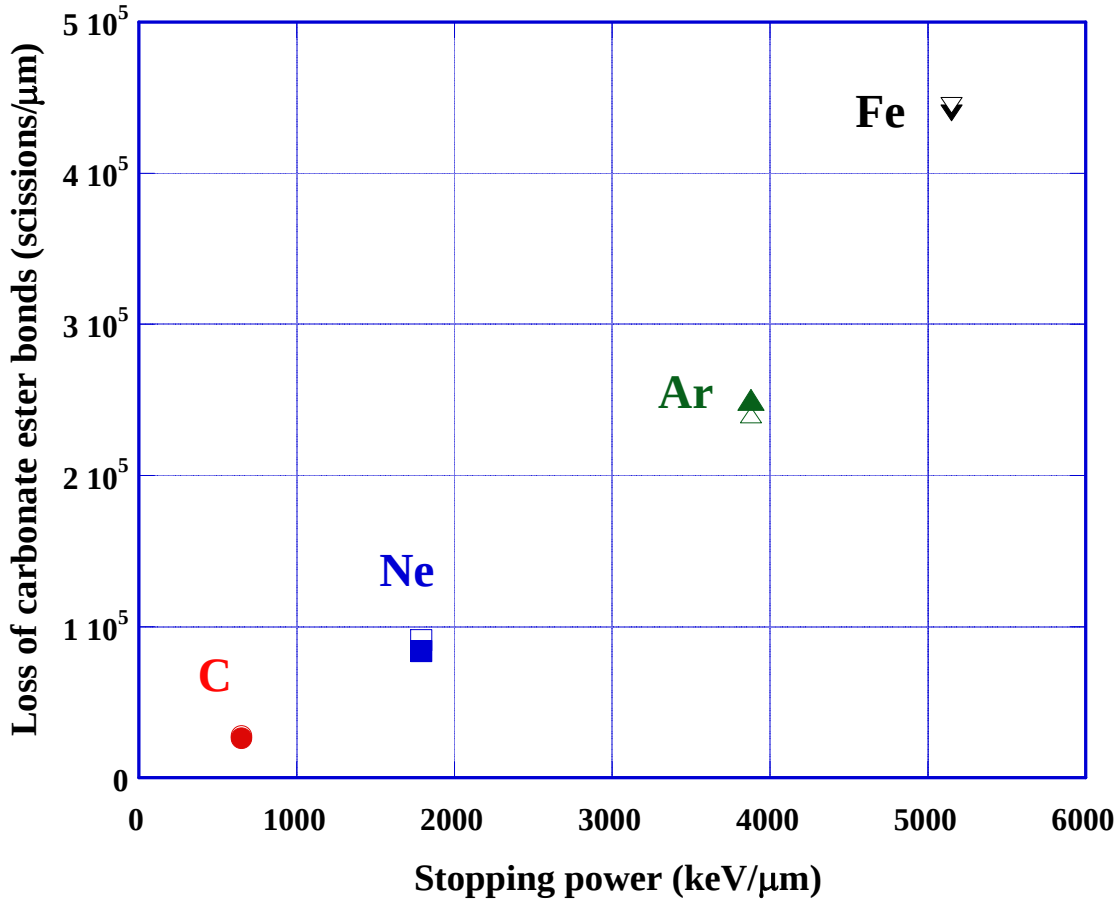

Fig. 4 Loss of carbonate ester bonds per unit length of ion tracks, damage density, as a function of the average stopping power of the PADC films. The values of solid symbols were estimated from C=O and the open ones from C-O-C.

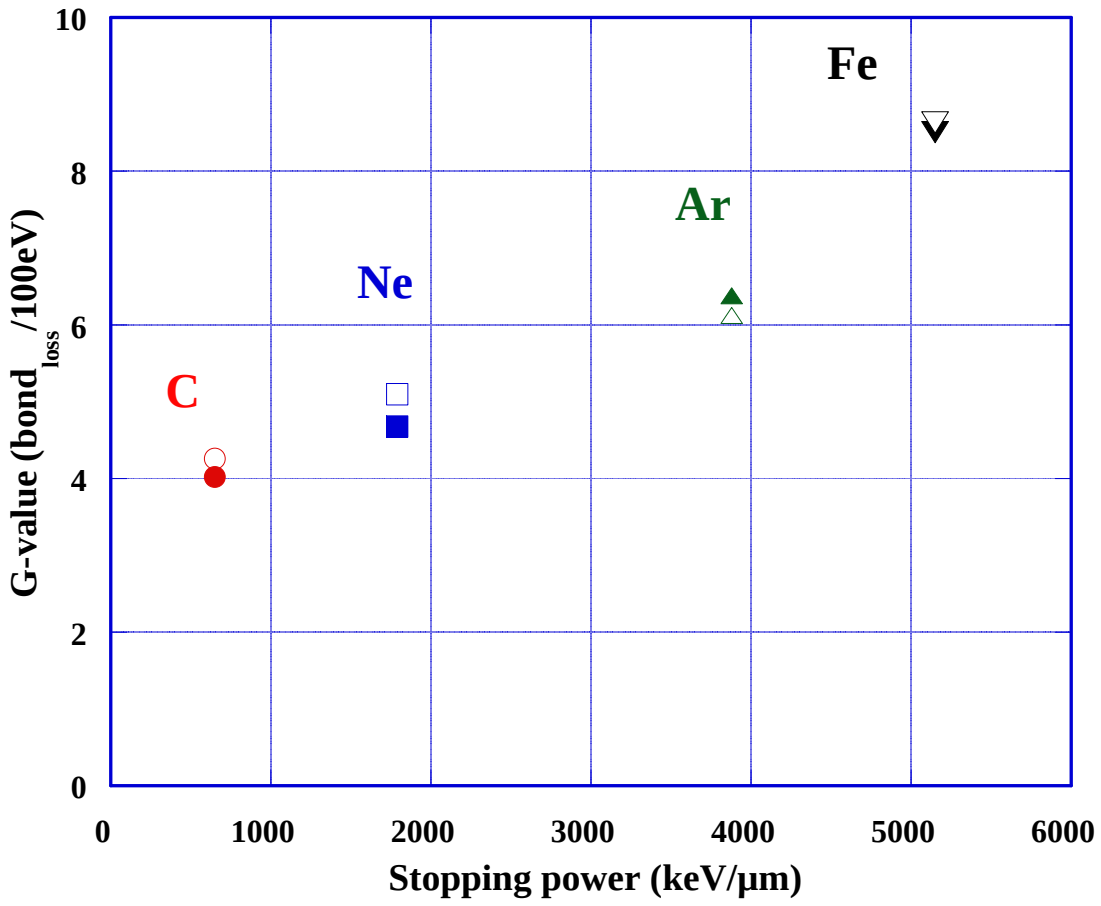

Fig. 5 G-values for the loss of carbonate ester bonds with the average stopping power. The values of solid symbols were estimated from C=O and the open ones from C-O-C.

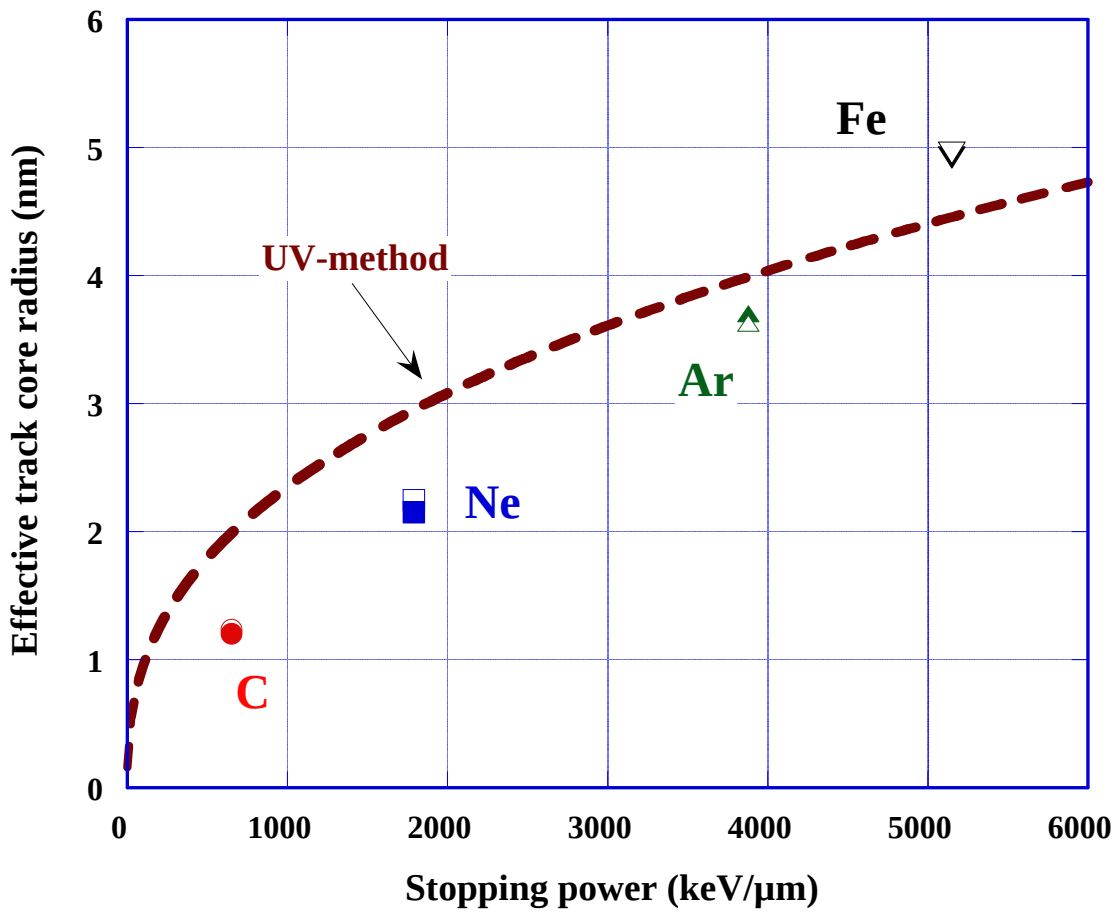

Fig. 6 Effective track core radius for the loss of carbonate ester bonds. The values of solids symbols were estimated from C=O and the open ones from C-O-C.

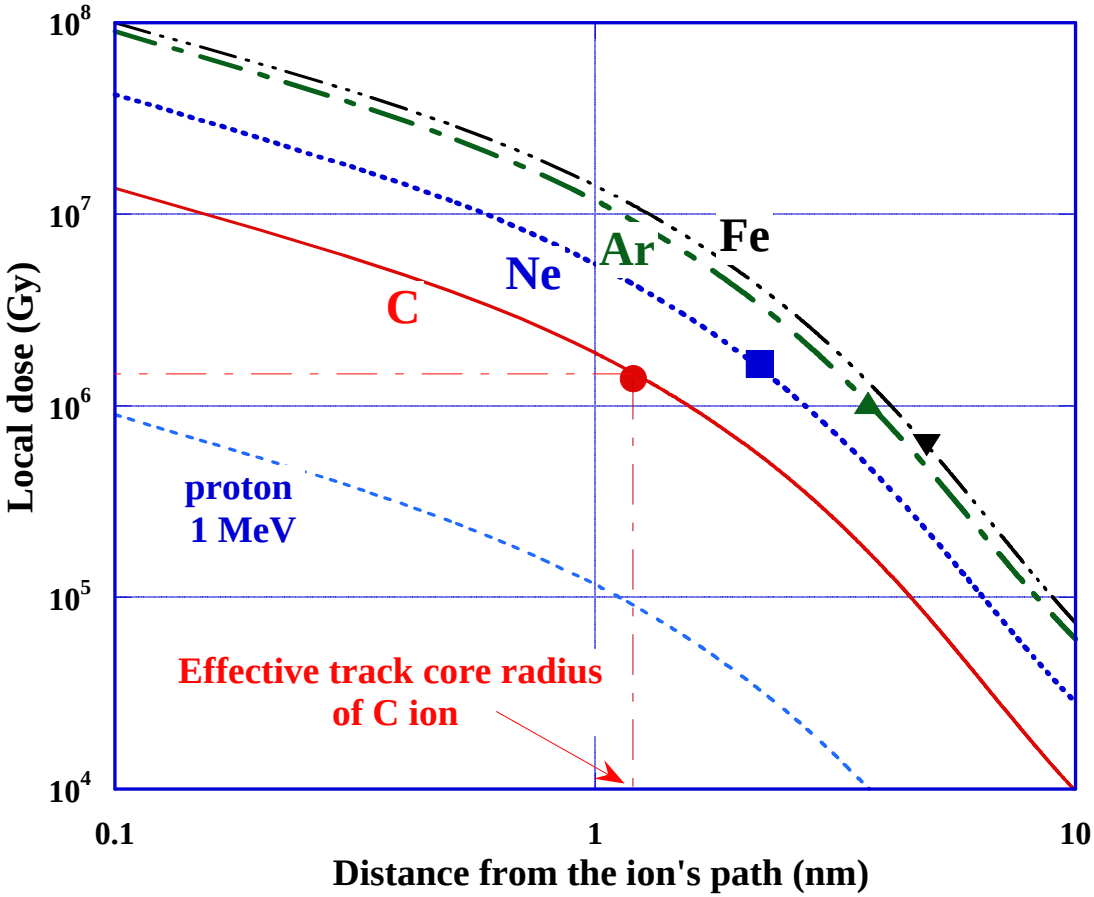

Fig. 7 Radial dose distribution of energy deposited around the path of heavy ions and protons in PADC. In this calculation the ionizing potential was set at I = 70.1 eV.